

The Kinetics of Hydrolytic Polymerization of ϵ -Caprolactam

KAZUO TAI, HIROICHI TERANISHI, YOSHIHIRO ARAI, and TAKASHI TAGAWA, *Research and Development Center, Unitika Ltd., Kozakura, Uji, Kyoto, 611 Japan*

Synopsis

A method to determine the concentration of ϵ -aminocaproic acid (ACA) in poly- ϵ -caprolactam by high-pressure liquid chromatography is established. The polymerizations for initial water concentrations of 0.42, 0.82, and 1.18 mol/kg and temperatures of 230, 240, 250, 260, 270, and 280°C were performed and concentration-versus-time curves were obtained for ACA, ϵ -caprolactam (CL), and endgroups (EG). Each curve for ACA and EG has a maximum which increases monotonically in its value and shifts from right to left in position with increasing either the temperature or the initial water concentration. The reaction rates of CL, EG, and ACA were also evaluated numerically from the concentration data. The observed kinetic data were compared with those obtained by the numerical solution of the rate equations with Reimschuessel's kinetic constants. Good agreement is found in CL and EG concentrations but discrepancies in ACA concentration and rates are considerable, particularly in the early stage of the polymerization.

INTRODUCTION

Poly- ϵ -Caprolactam (nylon 6) is industrially produced by hydrolytic polymerization of ϵ -caprolactam (CL). Many investigations of this polymerization have been performed and published. Recently, extensive work for various aspects of the polymerization has been reported by Reimschuessel and co-workers.¹⁻⁴ They described the mechanism and kinetics of the polymerization and proposed the kinetic constants of the rate equations. Their constants,^{1,2} however, were determined without experimental data concerning ϵ -aminocaproic acid (ACA). They estimated the equilibrium ACA concentration from the equilibrium endgroup concentration and the number-average degree of polymerization by assuming a Flory-Schulz distribution. There are few kinetic data of ACA dealing with a sufficient variety of the polymerization condition except those of Hermans et al.⁵ for comparatively limited conditions. Thus, the effects of the temperature and initial water concentration on the behavior of ACA during the polymerization have not yet been clarified.

The quantitative analysis of ACA has been performed by paper chromatography,^{5,6} polarography,⁷ and gel chromatography,^{8,9} but these methods seem to be lacking either rapidity or accuracy. In this work, a rapid and reliable method to determine ACA by high-pressure liquid chromatography is established, and kinetic data for ACA as well as CL and amino and carboxyl endgroups (EG) are obtained for various polymerization conditions. The observed data are compared with those of the solutions of the rate equations by using Reimschuessel's constants.² The purpose of this work is to clarify the behavior of ACA during polymerization and to test the applicability of Reimschuessel's constants for computer simulation of the polymerization.

EXPERIMENTAL

Polymerization

Molten CL containing prescribed concentration of water was pipetted into calibrated polymerization tubes (inside diameter 8 mm, 5 ml) at 80°C under nitrogen atmosphere. The concentration of water was determined by the Karl Fisher method. The tubes were quenched by Dry Ice-methanol and sealed under vacuum (10^{-3} Torr) in such a manner that only a negligible free volume existed after the mixture was heated to the temperature of the polymerization, after first measuring the thermal expansion of the material.

Polymerization was performed by heating the reaction tubes at the required temperatures for the required length of time. To standardize the procedure for heating the reactants to the polymerization temperature, a set of tubes was totally immersed in a salt bath of $\text{NaNO}_3/\text{KNO}_3$ (weight ratio 1/1) thermostated to $\pm 0.5^\circ\text{C}$, and then each sample tube was withdrawn from the bath at specific time intervals which were determined by yield-versus-time curves obtained by preliminary calculation of the rate equations. The sample tube was then quenched in water and preserved in a freezer.

Analyses

Analytical Procedures

The rod-shaped polymer samples were crushed to powder by a hammer or shaved by an electric pencil shaver. The weighted samples were then extracted with 20 times their weight of freshly distilled water at 80°C for 4 hr using sealed extraction tubes, after which they were filtered onto weighted glass filters and dried to constant weight by heating to 70°C under high vacuum. Under these conditions extraction equilibrium can be achieved and the hydrolysis of CL to ACA is negligibly small. The total hot water-soluble content was equal to the loss in weight of the sample caused by extractions. The contents of CL and ACA in aqueous solution were determined by a chromatographic method as described below.

ϵ -Aminocaproic Acid

ACA was analyzed by high-pressure liquid chromatography (HLC). The aqueous solution of the water-soluble components was chromatographed by using a Shimadzu-DuPont Model 830 HLC apparatus equipped with an ultraviolet spectrophotometer. A 200-nm wavelength was selected. The separation column was a μ -Bondapak C_{18} (Waters Associates), and the mobile phase was 0.1 mol/l. aqueous solution of NaH_2PO_4 (flow rate 2 ml/min). A chromatogram for ACA is shown in Figure 1. Here, the retention time of ACA is 4 min. The other water-soluble components such as CL and linear and cyclic oligomers, having longer retention times (CL, 51 min and linear dimer, 62 min) were released by applying the gradient method with isopropanol.



Fig. 1. High-pressure liquid chromatography of ACA.

ϵ -Caprolactam and Endgroups

A Shimadzu Model GC-6A gas chromatograph (GC) equipped with a dual-flame ionization detector was used for the analyses of CL. The GC was fitted with stainless-steel columns 1 m long packed with Tenax GC of 80/60 mesh (AKZO), and nitrogen was used as the carrier gas. In the analysis the oven temperature was set at 210°C and the carrier gas at 60 ml/min. Diethylene glycol was used as the internal standard.

Carboxyl endgroups were determined by titrating a 2% polymer solution in benzyl alcohol at 180°C with a 0.05 mol/l. KOH benzyl alcohol solution. Amino endgroups were determined by titrating a 1% polymer solution in *m*-cresol at room temperature with a 0.05 mol/l. aqueous solution of *p*-toluenesulfonic acid. The average of both was used as the EG concentration.

RATE EQUATIONS AND CALCULATION

Mechanism and Kinetics

Based upon investigations^{1-5,10-12} on the hydrolytic polymerization kinetics, the mechanism of the polymerization has been elucidated and the following description can be given. During the polymerization three main equilibrium reactions occur: (1) ring opening, (2) polycondensation, and (3) polyaddition; they are shown in Table I. Other secondary reactions such as cyclization have not been considered.

From the mechanism of reactions (1), (2), and (3) (Table I), some authors have derived sets of rate equations summarized in Table II, assuming that the reactivities of all carboxyl and amino endgroups are equal, independent of chain length. Here, x , y , z , z_2 , and w are concentrations (moles/kg) of CL, EG, ACA, linear dimer, and water, respectively, and the subscript 0 means initial concentrations. k_1 , k_2 , and k_3 are the rate constants, and K_1 , K_2 , and K_3 are equilibrium constants. The rate equations of set I were derived by Hermans et al.,⁵ Kruissink et al.,¹⁰ and Wiloth^{11,12} and developed and widely used by the group of Reimschuessel.¹⁻⁴ Equation (3') of set II reported by Mochizuki and Ito⁹ does not include a term due to reaction (3) of polyaddition, and the second term of the

TABLE I
 Equilibrium Reactions

1. Ring Opening	$\text{CL} + \text{H}_2\text{O} \rightleftharpoons \text{ACA}$ $x \quad w_0 - y \quad z$
2. Polycondensation	$\text{S}_n + \text{S}_m \rightleftharpoons \text{S}_{n+m} + \text{H}_2\text{O}$ $\text{—NH}_2 + \text{HOCO—} \rightleftharpoons \text{—NHCO—} + \text{H}_2\text{O}$ $y \quad y \quad x_0 - x - y \quad w_0 - y$
3. Polyaddition	$\text{CL} + \text{S}_n \rightleftharpoons \text{S}_{n+1}$ $x \quad y \quad y - z$

 TABLE II
 Rate Equations

Set I	$dx/dt = -k_1[x(w_0 - y) - z/K_1] - k_3[xy - (y - z)/K_3] \quad (1)$ $dy/dt = k_1[x(w_0 - y) - z/K_1] - k_2[y^2 - (x_0 - x - y)(w_0 - y)/K_2] \quad (2)$ $dz/dt = k_1[x(w_0 - y) - z/K_1] - 2k_2[yz - (y - z)(w_0 - y)/K_2] - k_3(xz - z_2/K_3) \quad (3)$
Set II	$\text{equations (1) and (2)} \quad (1, 2)$ $dz/dt = k_1[x(w_0 - y) - z/K_1] - 2k_2[yz - z(x_0 - x - y)(w_0 - y)/K_3y] \quad (3')$
Set III	$\text{equation (1)} \quad (1)$ $dy/dt = k_1[x(w_0 - y) - z/K_1] - k_2[y^2/2 - (y - z)(w_0 - y)/K_2] \quad (2'')$ $dz/dt = k_1[x(w_0 - y) - z/K_1] - k_2[yz - (y - z)(w_0 - y)/K_2] - k_3(xz - z_2/K_3) \quad (3'')$

right side of the equation seems to not be entirely valid. Equations of set III of Tirrell et al.¹³ were derived by introducing the discrete transformation to the molecular rate equations. In their process of derivation it is assumed that the hydrolysis of polymer, i.e., the reverse reaction of the polycondensation, is proportional to the concentration of the polymer. This assumption, however, is not valid since the experimental studies¹⁴ of hydrolysis of some polyamides showed that the hydrolysis reaction is proportional to the concentration of amide linkages. In addition, some questions are found in the probability terms of the rate equations. In the present study the rate equations of set I were used for the numerical calculations.

Numerical Calculation

Solution of Rate Equations

To solve the set of rate equations numerically, it is necessary to represent z_2 of the last term of eq. (3) as a function of x , y , and z . Three assumptions, (a)² $z_2 = z$, (b) $z_2 = (x_0 - x)(z/x_0)$ (Flory-Schulz distribution), and (c)¹⁵ $z_2 = (y - z)^2/(x_0 - x - y)$, were tested by preliminary calculations, the result being that no significant deviations were found among the solutions. Therefore, assumption (a) was used.

It seems to be generally accepted that the reactions are all catalyzed by the carboxyl endgroups, though Giori and Hayes¹⁶ concluded from a study of the polycondensation kinetics that the reaction follows a second-order mechanism. The rate constants can be written as follows:

$$k_i = k_i^0 + k_i^c y \quad (i = 1, 2, 3) \quad (4)$$

All these constants k_i^j depend on temperature T , for which the Arrhenius relations can be assumed:

$$k_i^j = A_i^j \exp(-E_i^j/RT) \quad (j = 0, c) \quad (5)$$

The equilibrium constants are expressed as a function of T :

$$K_i = \exp[(S_i - H_i/T)/R] \quad (6)$$

Here, A_i^j , E_i^j , S_i , H_i , and R are frequency factor, activation energy, entropy, enthalpy, and gas constant, respectively. A set of values of these constants reported by Reimschuessel² (Table III) was used for the calculations.

The rate equations were integrated numerically using the Runge-Kutta-Gill integration scheme with variable time increments ($1/64$, $1/128$, or $1/256$ hr) to prevent divergence. Calculations were carried out in a HITAC 8250 computer.

Evaluation of Experimental Data

The experimental reaction rates ($x' = dx/dt$, $y' = dy/dt$, and $z' = dz/dt$) were evaluated by numerical differentiation of the concentration-versus-time curves [$x(t)$, $y(t)$, and $z(t)$] obtained directly from the kinetic runs. To prevent scattering, the concentration curves were smoothed five times by a five-point smoothing formula before differentiation, since both the concentration and the

TABLE III
Kinetic Constants of the Rate Equations^a

i^b	j^c	A_i^j	E_i^j	H_i	S_i
1	0	1.694×10^6	2.1040×10^4	2.1142×10^3	-7.87×10^0
	c	4.106×10^7	1.8753×10^4		
2	0	8.687×10^9	2.2550×10^4	-6.1404×10^3	0.93×10^0
	c	2.337×10^{10}	2.0674×10^4		
3	0	2.620×10^9	2.1269×10^4	-4.0283×10^3	-6.95×10^0
	c	2.372×10^{10}	2.0400×10^4		

^a Taken from reference 2; A_i^0 ($\text{kg}/\text{mol}^2 \cdot \text{hr}$), A_i^c ($\text{kg}^2/\text{mol} \cdot \text{hr}$) E_i^j (cal/mol), H_i (cal/mol), S_i (e.u.).

^b $i = 1$, ring opening; $i = 2$, polycondensation; $i = 3$, polyaddition.

^c $j = 0$, uncatalytic; $j = c$, catalytic.

rate curves are essentially smooth. The first derivatives of the tabulated functions were computed at all points of the tables spaced $\frac{1}{8}$ hr by five-point differentiation formula. Then the rate functions were smoothed five times.

To show the degree of fitting between experimental and calculated concentration or rate curves, the following discrepancy factor (*DF*)

$$DF(\%) = 100 \sum_t |X(t)^{\text{obsd}} - X(t)^{\text{calcd}}| / \sum_t |X(t)^{\text{obsd}}| \quad (7)$$

was used, where *X* is *x*, *y*, *z*, *x'*, *y'*, or *z'* and *t* covers from 0 to 10 hr with increments of $\frac{1}{4}$ hr.

RESULTS AND DISCUSSION

Experimental Results

In this investigation the polymerizations were carried out at 230, 240, 250, 260, 270, and 280°C applying initial water concentrations of 0.42, 0.82, and 1.18 mol/kg. The results of these experiments (before smoothing) are given in Figures 2, 3, and 4. In Figure 5, for example, are shown the experimental reaction rates for the initial water concentration of 0.82 mol/kg which are evaluated from the corresponding concentration-versus-time curves.

The broken line in Figure 3(c) is an ACA concentration curve reported by Hermans et al.⁵ They analyzed ACA by paper chromatography for a series of samples polymerized at 221.5°C and an initial water concentration of 0.87 ml/kg. Considering the experimental uncertainty due to the quantitative analysis by paper chromatography, their curve is well consistent with this work.

Effect of Temperature and Initial Water Concentration

Figures 2, 3, and 4 suggest that the polymerization temperatures and initial water concentrations affect the concentration-versus-time curves of CL, EG, and ACA [*x*(*t*), *y*(*t*), and *z*(*t*)]. The curves *y*(*t*) and *z*(*t*) have a maximum. The maximum position t_{max} shifts from right to left, and the maximum concentrations y_{max} and z_{max} increase with rise of the polymerization temperature. The equilibrium concentrations of x_{equil} , y_{equil} , and z_{equil} also increase with temperature. The effect of initial water concentration on the *x*(*t*), *y*(*t*), and *z*(*t*) curves is similar to that of the polymerization temperature, as seen from Figure 6.

As for the reaction rates shown in Figure 5, *x'*(*t*) has a minimum and *y'*(*t*) and *z'*(*t*) have a maximum and a minimum. The maximum of *z'*(*t*) is not clear in Figure 5(c) because of insufficient experimental data of *z*(*t*) at the initial stage of the polymerization. These maximum and minimum points show a characteristic movement with variation of temperature or initial water concentration.

Calculated Concentration and Rate Curves

The observed concentration and reaction rate curves are compared with those of the calculations obtained by numerical solutions of rate equations using Reimschuessel's constants. Examples for the concentrations and rates are shown

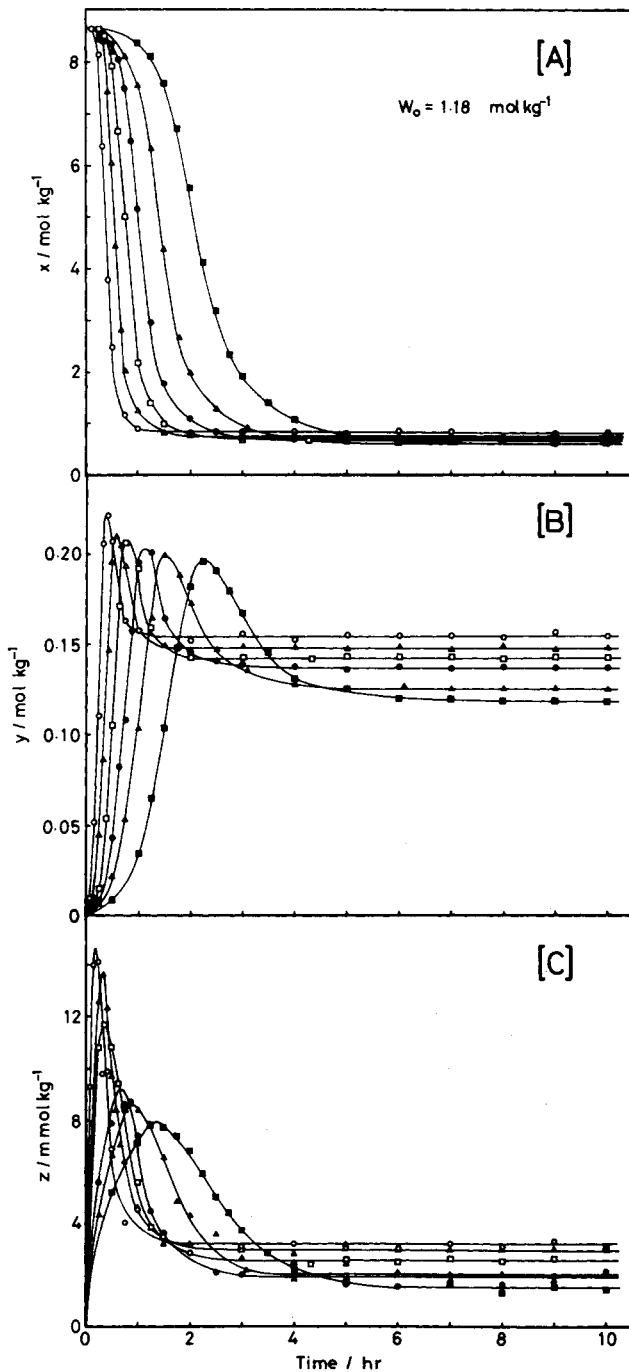


Fig. 2. Experimentally obtained concentration-vs-time curves for initial water concentration of 1.18 mol/kg and polymerization temperatures of (-■-) 231, (-▲-) 241, (-●-) 250, (-□-) 260, (-Δ-) 269, and (-○-) 281 °C: [A] CL curves $[x(t)]$; [B] EG curves $[y(t)]$; [C] ACA curves $[z(t)]$.

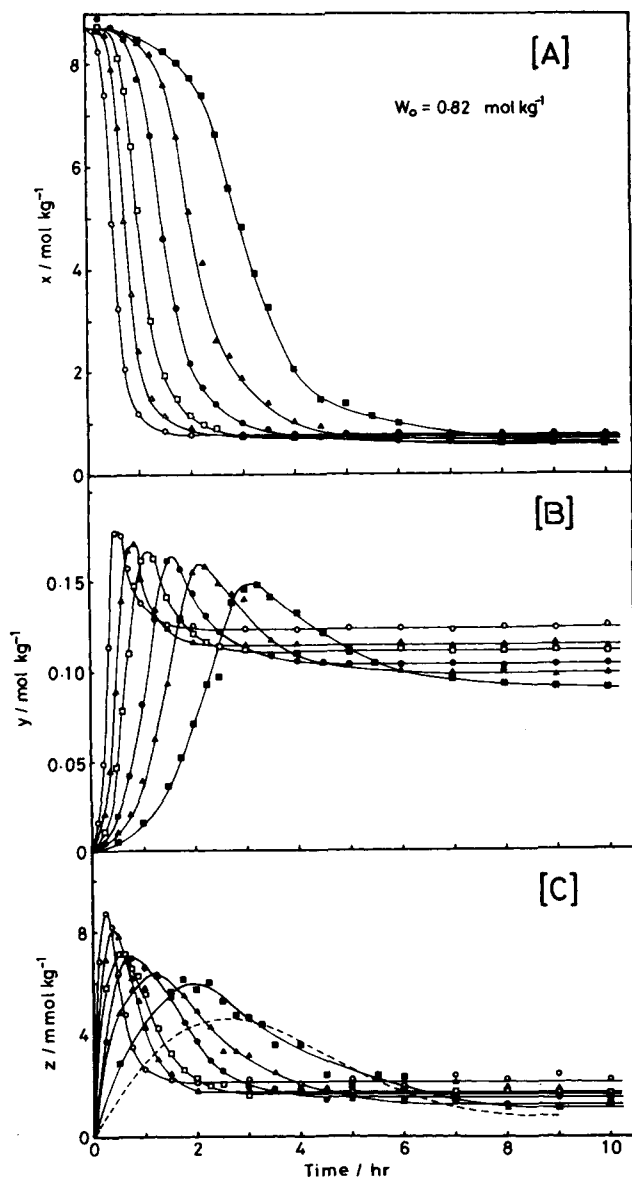


Fig. 3. Experimentally obtained concentration-vs-time curves for initial water concentrations of 0.82 mol/kg and polymerization temperatures of (-■-) 230, (-▲-) 240, (-●-) 249, (-□-) 259, (-△-) 269, and (-○-) 280°C: [A] CL curves $[x(t)]$; [B] EG curves $[y(t)]$; [C] ACA curves $[z(t)]$.

in Figures 7 and 8, where the polymerization temperature is 259°C and the initial water concentration is 0.82 mol/kg. The solid lines are the observed curves and the broken lines the calculated ones. Discrepancy factors (DF) are written in the figures. For the concentration curves of $x(t)$ and $y(t)$, sufficiently good agreement was found in the order of $DF = 5.7\%$ and 8.5% , though some discrepancy was found in $y(t)$ at the maximum position. In the case of $z(t)$, the DF value is as large as 32.0%, and considerable disagreement was found at the early stage of the polymerization. DF values for the reaction rate curves are

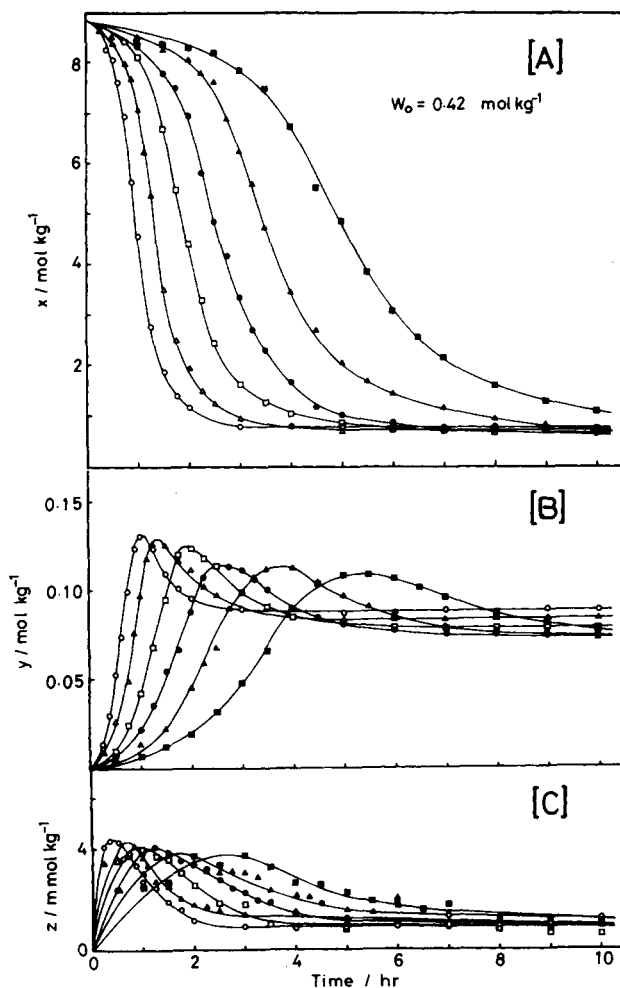


Fig. 4. Experimentally obtained concentration-vs-time curves for initial water concentration of 0.42 mol/kg and polymerization temperatures of (-■-) 231, (-▲-) 241, (-●-) 250, (-□-) 260, (-△-) 270, and (-○-) 280°C: [A] CL curves $[x(t)]$; [B] EG curves $[y(t)]$; [C] ACA curves $[z(t)]$.

larger than those of the concentration curves as shown in Figure 8, since the rate curves strongly reflect the early stage of the polymerization.

The discrepancy factors for concentration and rate curves of all kinetic runs are summarized in Table IV. The DF values of z' at 280°C for all initial water concentrations and of x' and y' at 280°C for initial water concentration of 1.18 mol/kg are absent from the table because of the following reason: The six observed rate curves have an appreciable uncertainty and cannot be compared with the calculations, since the corresponding experimental concentration curves have a steep-up-down or down at the early stage of the polymerization, and the numerical differentiation cannot follow it. From the table it can be pointed out that the observed and calculated $x(t)$ and $y(t)$ curves agreed well but that $z(t)$ and the rate curves did not.

The calculated $y(t)$ and $z(t)$ curves are plotted in Figure 9. The maximum position (t_{\max}) shifts from right to left with increasing polymerization temper-

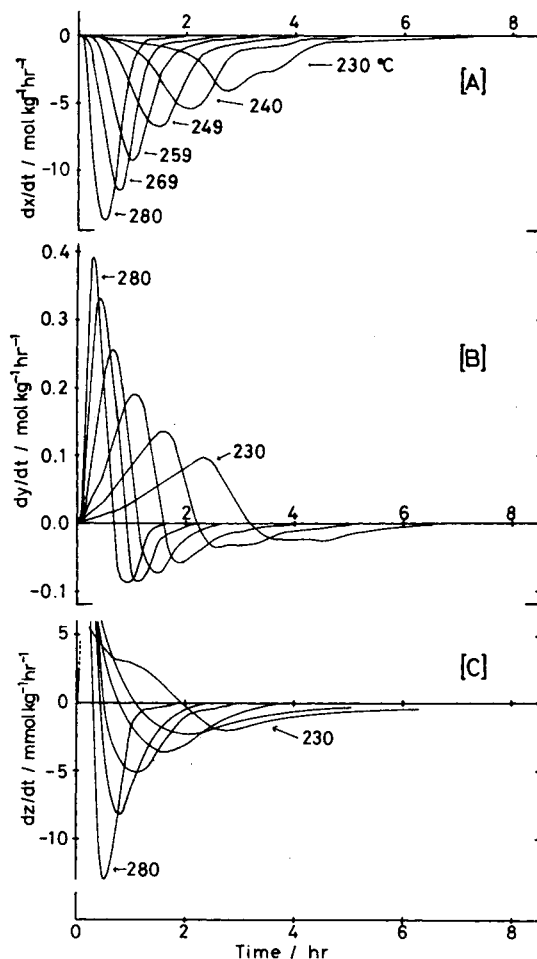


Fig. 5. Effect of temperature on reaction rate-vs-time curve for initial water concentration of 0.82 mol/kg: [A] CL rate curves $[x'(t)]$; [B] EG rate curves $[y'(t)]$; [C] ACA rate curves $[z'(t)]$.

ature in both cases. The maximum concentrations y_{\max} and z_{\max} , however, do not rise with the temperature in contrast to the observed curves shown in Figure 3. The reasons for this fact are not clear, but imperfections of the reaction mechanisms and the constants of the rate equations may be involved.

Constants of the Rate Equations

The equilibrium constants K_1 (ring opening), K_2 (polycondensation), and K_3 (polyaddition) calculated from x_0 , w_0 , x_{equil} , y_{equil} , and z_{equil} of these kinetic runs were in fair agreement with those of Reimschuessel,¹ in spite of the approximation of the z_{equil} by the Flory-Schulz distribution; $z_{\text{equil}} = y_{\text{equil}} P_n^{-1}$. For example, the observed z_{equil} and the evaluated z_{equil} for the initial water concentration of 0.82 mol/kg and the temperature of 259°C are 1.72 and 1.49 mmol/kg, respectively. The observed value is larger than the evaluated one by 12% in average for all the kinetic runs. The dependence of K_2 upon the initial water concentration is also consistent with the work of Reimschuessel.

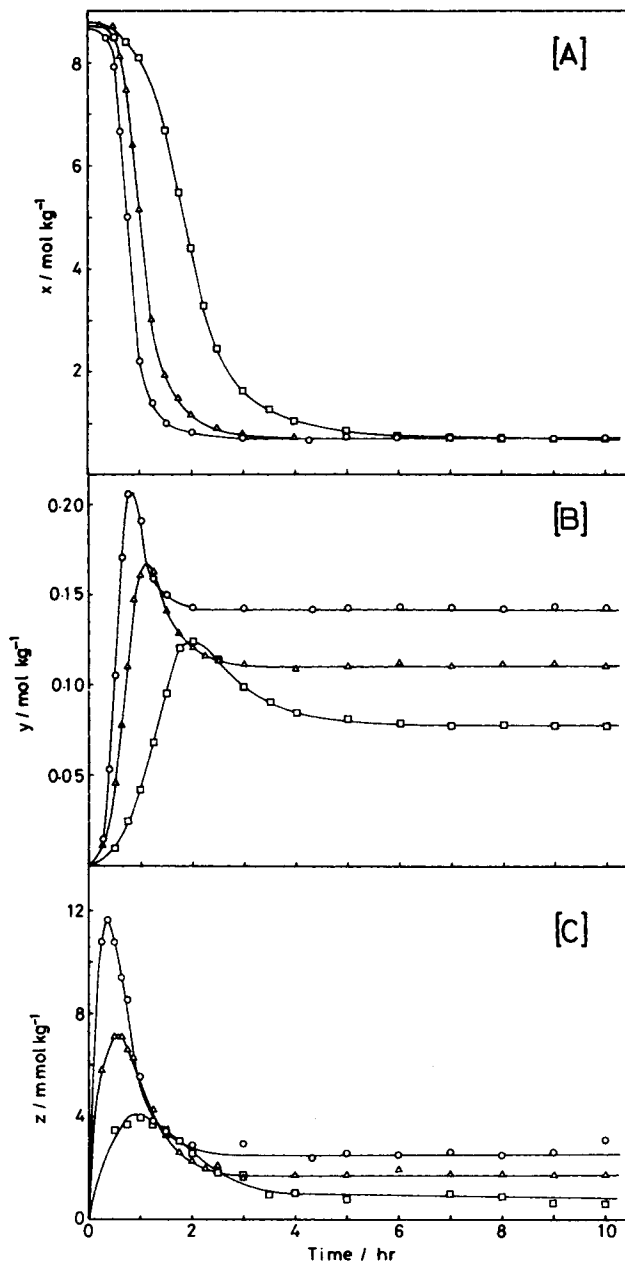


Fig. 6. Effect of initial water concentration on concentration-vs-time curve for polymerization temperature of 260°C: [A] CL curves; [B] EG curves; [C] ACA curves: initial concentration of water: (-O-) 1.18 mol/kg; (-Δ-) 0.82 mol/kg; (-□-) 0.42 mol/kg.

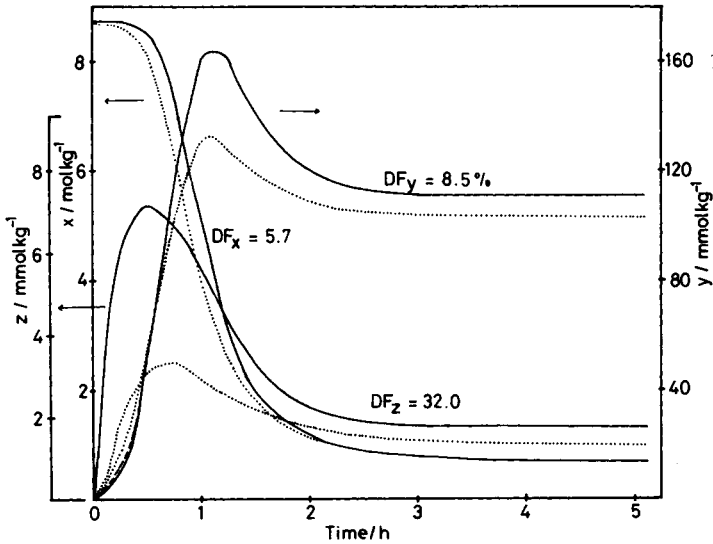


Fig. 7. Comparison of observed (—) and calculated (.....) concentration curves (using Reimschuessel's kinetic constants) of CL, EG, and ACA for initial water concentration of 0.82 mole/kg and the temperature of 259°C. The DF values are the discrepancy factors defined in the text.

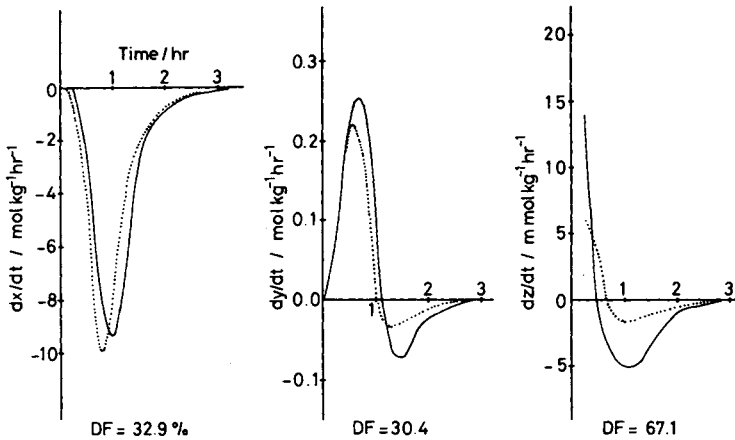


Fig. 8. Comparison of observed (—) and calculated (.....) reaction rate curves (using Reimschuessel's kinetic constants) of CL, EG, and ACA for initial water concentration of 0.82 mol/kg and the temperature of 259°C. The DF values are the discrepancy factors defined in the text.

The Reimschuessel constants, as discussed in the preceding section, gave rather large discrepancies between observed and calculated rate curves at the early stage of the polymerization. Thus, it may be expected that the fairly large errors are allowed for the simulation calculations of the polymerization by continuously stirred tank reactor (CSTR) with residence times (θ) of less than 5 hr, since the density distribution function $E(\theta)$ for CSTR has a significant weight for the early stage of the polymerization. For a more precise simulation, therefore, a re-evaluation of the kinetic constants appears to be in order and may involve the least-squares curve fitting technique proposed by Gerdes et al.¹⁵ The least-squares curve fitting using these kinetic runs is now in progress, and the results will be published elsewhere.

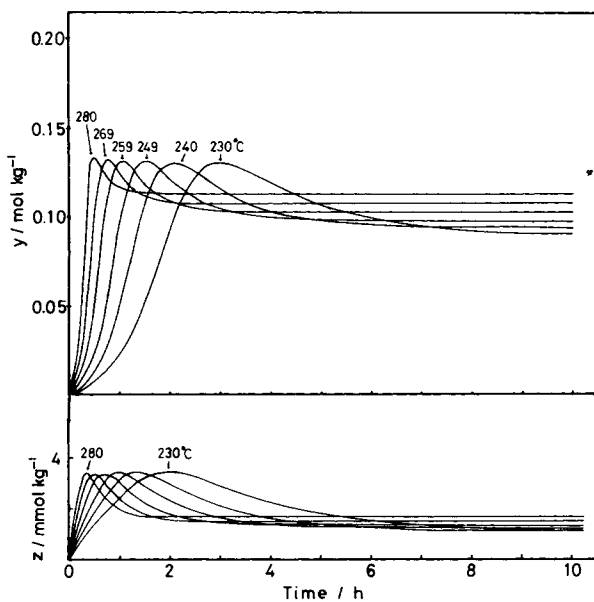


Fig. 9. Calculated concentration-vs-time curves of EG and ACA for initial water concentration of 0.82 mol/kg. The temperature was changed as shown on the curves.

TABLE IV
Discrepancies Between Observed and Calculated Kinetic Data

W_0	Temp., °C	Discrepancy factor, %					
		Concentrations			Rates		
		x	y	z	x'	y'	z'
0.42	231	4.6	13.7	47.0	26.3	35.5	71.0
	241	5.8	12.5	49.0	32.3	40.1	73.0
	250	7.5	10.0	48.6	36.1	39.5	78.1
	260	9.2	13.3	40.8	44.1	52.6	74.4
	270	9.9	12.9	45.1	44.5	43.5	74.8
	280	10.5	12.3	31.6	45.5	45.2	—
0.82	230	6.4	6.6	30.9	34.8	40.3	49.7
	240	6.9	8.1	30.9	36.4	41.9	57.8
	249	7.0	7.5	34.2	34.7	42.8	63.2
	259	5.7	8.5	32.0	32.9	30.4	67.1
	269	6.8	6.5	26.5	40.7	34.9	64.6
	280	7.8	9.3	26.7	22.5	49.9	—
1.18	231	6.1	11.2	21.2	36.3	45.1	39.9
	241	5.5	10.8	25.0	34.9	43.4	47.4
	250	6.1	11.3	15.8	33.5	38.9	43.6
	260	7.4	11.1	31.3	44.3	35.1	56.1
	269	6.2	11.3	32.6	30.1	46.2	58.2
	281	4.6	12.5	26.9	—	—	—

References

1. H. K. Reimschuessel, in *Ring-Opening Polymerization*, K. C. Frisch and S. L. Reegen, Eds., Marcell Dekker, New York, 1969, Chap. 7, p. 303.
2. H. K. Reimschuessel and K. Nagasubramanian, *Chem. Eng. Sci.*, **27**, 1119 (1972).
3. H. K. Reimschuessel and K. Nagasubramanian, *Polym. Eng. Sci.*, **12**, 179 (1972).

4. H. K. Reimschuessel, *J. Polym. Sci. Macromol. Rev.*, **12**, 65 (1977).
5. P. H. Hermans, D. Heikens, and P. F. Van Velden, *J. Polym. Sci.*, **30**, 81 (1958).
6. H. Yumoto and N. Ogata, *Makromol. Chem.*, **25**, 91 (1958).
7. T. A. Robinson, *Anal. Chem.*, **39**, 836 (1967).
8. S. Mori and T. Takeuchi, *J. Chromatogr.*, **50**, 419 (1970).
9. S. Mochizuki and N. Ito, *Chem. Eng. Sci.*, **28**, 1139 (1973).
10. C. A. Kruissink, G. M. Van Der Want, and A. J. Staverman, *J. Polym. Sci.*, **30**, 67 (1958).
11. F. Wiloth, *Kolloid-Z.*, **143**, 129 (1955); *ibid.*, **144**, 58 (1955).
12. F. Wiloth, *Z. Phys. Chem. Neue Folge*, **11**, 78 (1957).
13. M. V. Tirrell, G. H. Person, R. A. Weiss, and R. L. Laurence, *Polym. Eng. Sci.*, **15**, 386 (1975).
14. D. Heikens, *J. Polym. Sci.*, **22**, 65 (1956); *ibid.*, **35**, 277 (1959).
15. F. O. Gerdes, P. J. Hoftyzer, J. F. Kemkes, M. Van Loon, and C. Schweibman, *Chem. Eng.*, CE267 (1970).
16. C. Giori and B. T. Hayes, *J. Polym. Sci. A-1*, **8**, 335 (1970).

Received August 18 1978

Revised November 7, 1978